Basic Science and Experimental Studies

(Pro)renin Receptor Blockade Ameliorates Heart Failure Caused by Chronic Kidney Disease

AKIHIRO YOSHIDA, MD, HIROMITSU KANAMORI, MD, PhD, GENKI NARUSE, MD, SHINGO MINATOGUCHI, MD, PhD, MASAMITSU IWASA, MD, PhD, YOSHIHISA YAMADA, MD, PhD, ATSUSHI MIKAMI, MD, PhD, MASANORI KAWASAKI, MD, PhD, KAZUHIKO NISHIGAKI, MD, PhD, AND SHINYA MINATOGUCHI, MD, PhD

Gifu, Japan

ABSTRACT

Background: The (pro)renin receptor [(P)RR)] is involved in the activation of local renin-angiotensin system and subsequent development of cardiovascular disease. We investigated the therapeutic effect of a (P)RR blocker, handle-region peptide (HRP), on chronic kidney disease (CKD)−associated heart failure.

Methods and Results: CKD was induced in C57BL/6J mice by means of five-sixths nephrectomy. Eight weeks later, cardiac dysfunction and cardiac dilatation with hypertension developed. Mice were then assigned to 1 of the 3 following groups: vehicle, low-dose (0.01 $mg{\cdot}kg^{-1}{\cdot}d^{-1}$) HRP, or high-dose (0.3 $mg{\cdot}kg^{-1}{\cdot}d^{-1}$) HRP for 4 weeks. High-dose HRP treatment reversed left ventricular dilation and significantly improved cardiac dysfunction with ameliorated hypertension compared with the vehicle. The hearts with high-dose HRP treatment showed significant attenuation of cardiac fibrosis, cardiomyocyte hypertrophy, macrophage infiltration, and oxidative DNA damage. This treatment decreased the myocardial expressions of angiotensin (Ang) II, Ang II type 1 receptor, transforming growth factor β1, extracellular matrix−related proteins, and lipid peroxidation. Autophagy was activated in the cardiomyocyte from nephrectomized mice, but HRP treatment had no effect on cardiomyocyte autophagy.

Conclusions: This study indicates that (P)PR blockade is a beneficial strategy by suppressing cardiac fibrosis and hypertrophy to ameliorate heart failure caused by CKD. (*J Cardiac Fail 2019;25:286−300*)

Key Words: (Pro)renin receptor, chronic kidney disease, fibrosis, hypertrophy.

Chronic kidney disease (CKD) is a major worldwide public health problem and is now accepted as a major risk factor for cardiovascular morbidity and mortality.[1] Patients with CKD have a 10−30-fold greater risk of cardiac death compared with the general population.[2] Ischemic heart disease, heart failure, and cardiomyopathy are the most frequent causes of cardiac death in CKD patients. Cross-sectional studies indicate that left ventricular hypertrophy (LVH) is the most frequent cardiac alteration and an independent risk factor for survival in CKD patients.[3] LVH is initially an adaptive response to compensate for hemodynamic overload, subsequently developing into decompensated status or heart failure.[4] An LVH heart associated with CKD is usually accompanied by cardiomyocyte hypertrophy and diffuse interstitial fibrosis.[5] The renin-angiotensin system (RAS) contributes to LVH through the angiotensin II type 1 receptor (AT1R) and plays a pivotal role in the development of heart failure related to CKD.[6,7] RAS involves 2 pathways: circulating RAS and tissue RAS; the former is a classic endocrine system that regulates cardiovascular homeostasis during a physiologic and pathologic state through modulating arterial blood pressure and sodium homeostasis; the latter is attributed to local angiotensin (Ang) II production. The locally produced Ang II plays an important role in cardiac remodeling in an autocrine or paracrine manner in various pathologic states, such as post−myocardial infarction remodeling.[8] We previously reported that cardiac-tissue RAS was activated in the hearts of CKD mice, and AT1R blockade by genetic or

From the Department of Cardiology, Gifu University Graduate School of Medicine, Gifu, Japan.

Manuscript received February 23, 2018; revised manuscript received December 20, 2018; revised manuscript accepted February 8, 2019.

Reprint requests: Hiromitsu Kanamori, MD, PhD, Department of Cardiology, Gifu University Graduate School of Medicine, 1-1 Yanagido, Gifu 501-1194, Japan. Tel: +81-58-230-6523; Fax: +81-58-230-6524. E-mail: hk1973@gifu-u.ac.jp

Funding: This study was supported in part by a Research Grant from Gifu University School of Medicine and Novartis Pharma research grants.

See page 298 for disclosure information.

1071-9164/$ - see front matter

https://doi.org/10.1016/j.cardfail.2019.02.009

pharmacologic intervention mitigated CKD-associated heart failure through suppressing cardiac hypertrophy and interstitial fibrosis.[9]

The recently identified functional receptor for renin and its precursor prorenin, the (pro)renin receptor [(P)RR], plays a pathophysiologic role in the continuously expanding RAS system.[10,11] The (P)RR, a 350-amino-acid single-transmembrane protein, is widely expressed in various organs, including the brain, heart, kidneys, liver, and skeletal muscle.[12] (P)RR interacts with prorenin to exert renin activity through the conformational change without conventional proteolysis. In addition to activating tissue RAS,[11] (P)RR has another intracellular signaling pathway, the p38 MAPK/HSP27 pathway, which alters actin filament dynamics[13] and may induce cardiac hypertrophy. In addition, (P)RR is an integral accessory protein of vacuolar-type H^+-adenosine triphosphatase (V-ATPase), which is an essential component for autophagy.[10] Because autophagy is a degradation mechanism to compensate for the lack of energy and maintain intracellular homeostasis,[14] (P)RR may have a significant role in CKD-associated heart failure. Indeed, cardiomyocyte-specific deletion of (P)RR resulted in heart failure with highly vacuolized cardiomyocytes, indicating impaired autophagic degradation.[15]

The recently developed (P)RR antagonist, "handle-region peptide" (HRP),[16] competes with the handle region of prorenin for binding to (P)RR and inhibits nonproteolytic activation of prorenin. A number of studies on the effects of (P)RR blockade have been conducted with the use of a variety of experiments including hypertensive cardiomyopathy,[17–19] pacing-induced heart failure,[20] and cardiac remodeling after myocardial infarction.[21,22] However, there have been few reports of the effect of (P)RR blockade on cardiac alteration in CKD. Here, we report the effect of (P)RR blockade with the use of HRP on CKD-associated heart failure and investigate the underlying molecular mechanism.

Methods

This study conforms to the Guide for the Care and Use of Laboratory Animals published by the US National Institutes of Health (8th ed, 2011) and was approved by the Institutional Animal Research Committee of Gifu University. Mice were housed in a humidity- and temperature-controlled environment with 12-hour light-dark cycles, and received food and water ad libitum.

Animal Model and Experimental Protocol

Mice were purchased from Chubu-Kagaku Co (Nagoya, Japan). The five-sixths kidney ablation was performed to induce renal failure, as previously described, in male C57BL/6J mice at the age of 8 weeks.[9] This entailed the initial removal of both poles of the left kidney followed by the removal of the entire right kidney 1 week later. Sham-operated animals underwent the same surgical procedure without nephrectomy. These operations were performed under combination anesthesia with halothane (induction, 2%; maintenance, 0.5%) in a mixture of N_2O and O_2 (0.5 L/min each) via a nasal mask.

We performed the five-sixths kidney ablation in 30 mice, of which 26 survived 8 weeks after the second operation (survival rate 87%). The surviving mice, deemed to have CKD, were assigned to 3 groups: saline solution−treated (control) group (n = 10); 0.01 $mg \cdot kg^{-1} \cdot d^{-1}$ (low-dose) HRP (IPLKKMPS designed as mouse HRP; Genedesign,[16,22,23] Osaka, Japan; n = 6); and 0.3 $mg \cdot kg^{-1} \cdot d^{-1}$ (high-dose) HRP (n = 10). The agents were administered for 4 weeks via an osmotic minipump (Alzet; Durect, Cupertino, California) implanted subcutaneously on the anterior back under the combination anesthesia. We used 2 doses of HRP (0.01 and 0.3 mg/kg) to assess the dose-dependent effects. Both doses were chosen based on previous studies and were reported not to cause apparent harmful effects in rodents.[16–19,21–23] To assess the effects of these treatments on mice without CKD, sham-operated mice were assigned as well 8 weeks after the second operation (n = 10, 6, and 10, respectively). All mice were examined 4 weeks after starting treatment (12 weeks after nephrectomy).

In addition, we used GFP-LC3 transgenic mice to monitor autophagic vacuoles in the same manner (n = 6 each). Pathogen-free heterozygous GFP-LC3 transgenic mice (strain GFP-LC3#53) (Riken Bioresource Center) harbored a rat GFP-LC3 fusion construct under the control of the chicken β-actin promoter.[24]

Physiologic Studies

Echocardiography, systolic blood pressure (SBP) measurement, and cardiac catheterization were performed as described previously with some modifications.[9,25] In brief, echocardiograms were recorded with the use of an echocardiographic system (Vevo 770; Visualsonics, Toronto, Ontario, Canada) equipped with a 45-MHz imaging transducer, and SBP was measured by means of the tail-cuff method (BP98-A; Softron Co, Tokyo, Japan) at 8 weeks after surgery and at subsequent treatment for 4 weeks. Because of its invasiveness, cardiac catheterization was performed just before the animal was killed; the right carotid artery was cannulated with a micromanometer-tipped catheter (FTH-1611B-0018; Transonic Science, London, Ontario, Canada) that was advanced into the aorta and then into the left ventricle to record pressure and maximal and minimal dP/dt. Echocardiography, cardiac catheterization, and blood sampling were performed under combination anesthesia before the mice were killed by draining their blood until the light reflex was lost.

Histologic Analysis

Once the physiologic measurements were complete, mice were killed and the hearts removed, weighed, and cut into 2 transverse slices through the middle of the ventricles, between the atrioventricular groove and apex. The

specimens derived from the basal portion of hearts were fixed in 10% buffered formalin, embedded in paraffin, cut into 4-μm-thick sections, and stained with hematoxylin-eosin, Masson trichrome, or Sirius red F3BA (0.1% solution in saturated aqueous picric acid; Sigma-Aldrich, St Louis, Missouri). Quantitative assessments and morphometric analyses were carried out in randomly chosen high-power fields (×400) in each section as previously described.[9,25] In brief, morphometric analysis of fibrosis was carried out with the use of a multipurpose color image processor (Win ROOF; Mitani Corp, Tokyo, Japan). The cardiomyocyte size was measured as the transverse diameter of the myocyte cut at the level of the nucleus, as previously reported.[26]

Immunohistochemistry and Immunofluorescence

After deparaffinization, the 4-μm-thick sections were incubated with a primary antibody against F4/80 (Bio-Rad, Hercules, California), 8-hydroxy-2′-deoxyguanosine (8-OHdG; Japan Institute of the Control of Aging, Shizuoka, Japan), ATP6P2/(P)RR (Abcam, Cambridge, Massachusetts), GFP (Thermo Fisher Scientific, Waltham, Massachusetts), or cathepsin D (Santa Cruz Biotechnology, Santa Cruz, California). A Vectastain Elite ABC system (Vector Laboratories, Burlingame, California) was used for immunostaining; diaminobenzidine served as the chromogen, and the nuclei were counterstained with hematoxylin. To observe autophagic activity in cardiomyocytes, sections immunostained with anti-GFP followed by Alexa Fluor 488 (green; Molecular Probes, Thermo Fisher Scientific KK, Japan) were also treated with antimyoglobin antibody (Dako, Japan) followed by Alexa Fluor 568 (red; Molecular Probes). These sections were then counterstained with Hoechst 3342 (Setareh Biotech) and observed under a confocal microscope (C2; Nikon, Tokyo, Japan). Quantitative assessments, including the number of immunopositive dots within cardiomyocytes, were performed in 20 randomly chosen high-power fields (×600) with the use of a multipurpose color image processor (BZ-Analyzer; Keyence, Osaka, Japan).

Electron Microscopy

The cardiac ultrastructure was examined by conventional method as previously described.[25] Cardiac tissue was quickly cut into 1-mm cubes, immersion fixed in 2.5% glutaraldehyde in 0.1 mol/L phosphate buffer (pH 7.4) overnight at 4°C, and postfixed in 1% buffered osmium tetroxide. The specimens were then dehydrated through a graded ethanol series and embedded in epoxyresin. Ultrathin sections (80 nm), double-stained with uranyl acetate and lead citrate, were examined under a transmission electron microscope (H-800; Hitachi, Tokyo, Japan).

Western Blotting Analysis

Proteins (50 μg) extracted from hearts were subjected to 7.5%, 10%, or 15% polyacrylamide gel electrophoresis and then transferred onto polyvinylidene difluoride membranes. The membranes were then probed with the use of primary antibodies against ATP6P2/(P)RR (Abcam), Ang II (Novus Biologicals, Littleton, Colorado), transforming growth factor (TGF)-β1 (Promega, Madison, Wisconsin), AT1R, tissue inhibitor of metalloprotease (TIMP) 1 (both from Santa Cruz Biotechnology), 4-hydroxyl-2-nonenal (4-HNE; NOF Corp, Tokyo, Japan), collagen I, matrix metalloproteinase (MMP) 2, MMP-9, V-ATPase (all 4 from Abcam), microtubule-associated protein 1 light chain 3 (LC3; MBL International, Nagoya, Japan), extracellular signal−regulated protein kinase (ERK), phosphorylated (p) ERK, p38 mitogen−activated protein kinase (p38MAPK), p-p38MAPK (all 4 from Cell Signaling), heat shock protein (HSP) 27, and p-HSP27 (both from Santa Cruz Biotechnology). The blots were visualized with the use of enhanced chemiluminescence (Amersham/GE Healthcare, Little Chalfont, UK). α-Tubulin (analyzed with the use of an antibody from Santa Cruz Biotechnology) served as the loading control. The protein content was expressed as a ratio (arbitrary units) relative to that of a loading control. Activations of ERK, p38MAPK, and HSP27 were assessed with the use of antibodies against their phosphorylated forms.

Serum Biochemical Measurement

Blood samples were collected from the carotid artery after catheter examination at the end of the experiment. The samples were used for the measurement of serum creatinine and blood urea nitrogen. They were measured at a clinical laboratory (SRL, Tokyo, Japan).

Measurement of Circulating RAS and Prorenin

Blood samples were collected from the carotid artery after catheter examination at the end of the experiment. Plasma renin activity (PRA) and plasma Ang II levels were measured by means of the RIA2 method at a clinical laboratory (SRL, Tokyo, Japan). The plasma total prorenin-renin level was quantified with the use of the Mouse Prorenin/Renin Total Antigen Assay Kit (Innovative Research, Plymouth, Massachusetts) according to the manufacturer's instructions.

Statistical Analysis

The data are expressed as mean ± SEM. The homogeneity of variances was evaluated by means of Levene test. All data were tested for normal distribution by means of Kolmogorov-Smirnov test. The significance of differences between groups was evaluated by means of 1-way analysis of variance (ANOVA) followed by Newman-Keuls multiple comparisons test for post hoc comparisons, or by repeated-measures ANOVA. Statistical analyses were performed with the use of Stat View version 5.0 (SAS Institute, Cary, North Carolina) and Excel 2013 (Microsoft, Redmond, Washington). P values of $<.05$ were considered to be significant.

Results

Survival and Renal Function

All mice in all groups survived the 4 weeks of treatment (12 weeks after operation). Serum creatinine and blood urea nitrogen levels were significantly elevated in the nephrectomized groups compared with the sham-operated groups. Neither the high-dose nor low-dose HRP affected the renal function in any group (Fig. 1A and 1B).

Hemodynamics

The systolic blood pressure (SBP) significantly increased in nephrectomized mice 8 weeks after the operation compared with sham-operated mice. High-dose (but not low-dose) HRP treatment for the subsequent 4 weeks reversed this increase in SBP similarly to sham-operated mice. In contrast, neither the high-dose nor low-dose HRP treatment affected SBP in sham-operated mice (Table 1; Fig. 1C and 1D).

Cardiac Function and Remodeling

Echocardiography and cardiac catheterization were performed to assess cardiac geometry and function. An enlarged left ventricular (LV) cavity and impaired LV function were noted in nephrectomized mice 8 weeks after the operation: the LV end-diastolic diameter was increased and LV ejection fraction reduced compared with sham-operated mice (Table 1; Fig. 1C). This LV dilation developed during the subsequent 4 weeks in the saline solution−treated mice. In contrast, mice treated with high-dose (but not low-dose) HRP showed a reduced LV cavity and improved cardiac performance: decreased end-diastolic pressure and improved maximal and minimal change in pressure over time (LV dP/dt) compared with saline solution−treated mice (Table 1; Fig. 1C and 1D). On the other hand, neither low- nor high-dose HRP treatment affected the cardiac geometry or performance in sham-operated mice.

Our physiologic studies revealed that only high-dose, not low-dose, HRP was effective, suggesting the dose-dependent effect of this peptide. Therefore, we performed subsequent mechanistic studies (histologic or biochemical analyses) with the use of only the group treated with high-dose, rather than low-dose, HRP.

Histologic and Immunohistochemical Findings in the Heart

The heart weight−body weight ratios in nephrectomized mice were significantly greater than in sham-operated groups, consistent with the cardiomyocyte hypertrophy (Fig. 2A and 2B). Sirius red staining showed significantly increased in myocardial interstitial fibrosis in the nephrectomized mice compared with the sham-operated mice (Fig. 2C). In addition, F4/80-positive macrophage infiltration into the myocardium was significantly increased in the nephrectomized mice (Fig. 2D). The DNA base-modified product 8-hydroxy-2′-deoxyguanosine (8-OHdG) is commonly known as a marker of oxidative DNA damage.[27] The incidence of 8-OHdG−positive cardiomyocytes was also markedly increased in the nephrectomized mice (Fig. 2E). All of these myocardium phenotypes induced by nephrectomy—hypertrophied cardiomyocytes, marked fibrosis, inflammatory cell infiltration, and oxidative damage—were significantly attenuated by HRP treatment in nephrectomized mice (Fig. 2A−2E).

In summary, nephrectomy caused cardiac hypertrophy, cardiomyocyte hypertrophy with an increase in fibrosis, macrophage infiltration, and oxidative damage in the heart. HRP treatment attenuated these deleterious findings.

Fibrosis Mediators and Lipid Peroxidation in the Heart

We next assessed the levels of fibrosis and oxidative damage−related molecules in the heart. TGF-β1 is one of the major key profibrotic cytokines mediating the remodeling of cardiac fibrosis and the extracellular matrix (ECM).[28] ECM was mediated by matrix metalloproteases (MMPs) or matrix metalloproteinase inhibitors (TIMPs): the former degrade ECM enzymatically, the latter inhibits the activity of the former.[29] Western blotting analysis revealed that myocardial expressions of TGF-β1, collagen I, MMP-2 (active isoform), MMP-9 (pro and active isoforms), and TIMP-1 were all significantly increased in hearts from nephrectomized mice compared with sham-operated mice (Fig. 3). All of these up-regulated protein levels were decreased in HRP-treated hearts of nephrectomized mice (Fig. 3). Western blotting analysis of 4-HNE, a marker of oxidative damage to the cell membrane,[30] showed that nephrectomy increased lipid peroxidation in the heart, whereas HRP treatment significantly reduced the level (Fig. 3).

Circulating RAS and Prorenin

PRA, Ang II, and total renin-prorenin levels were not different between sham-operated and nephrectomized mice and were not affected by HRP-treatment (Fig. 4A−4C).

(P)RR and RAS in the Heart

Western blotting revealed that the (P)RR expression levels were significantly increased in the hearts of nephrectomized mice compared with sham-operated mice and were not affected by HRP treatment (Fig. 4D). In immunohistochemistry, marked immunosignal for (P)RR was noted in cardiomyocytes from nephrectomized mice compared with sham-operated mice and was not affected by HRP treatment (Fig. 4D). Western blotting indicated that the levels of Ang II were significantly increased in the hearts of nephrectomized mice compared with sham-operated mice and was suppressed by HRP treatment (Fig. 5E). In addition, the AT1R expression levels paralleled those of heart tissue Ang II (Fig. 5E).

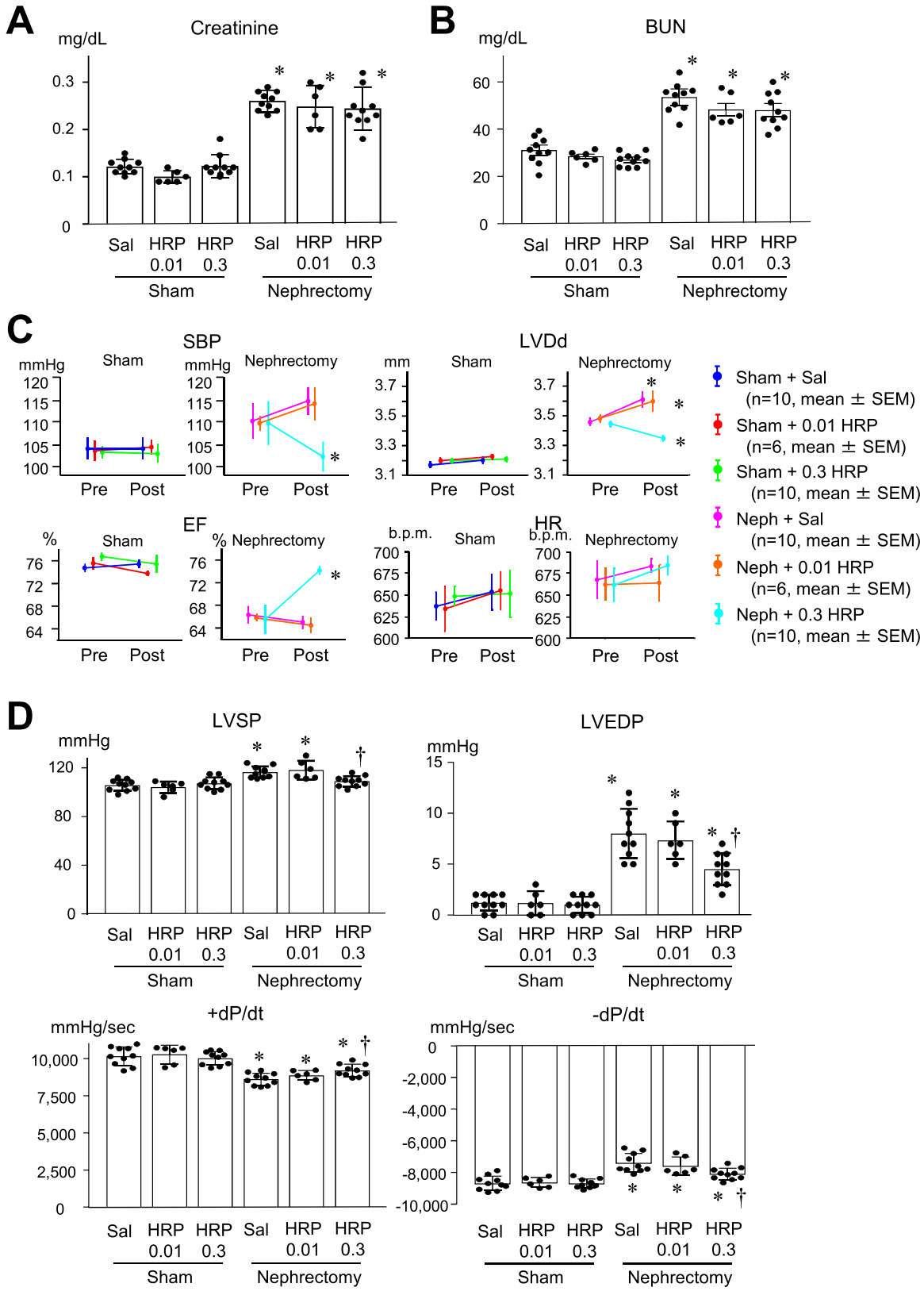

Fig. 1. Laboratory data and hemodynamic parameters. **(A)** Serum creatinine and **(B)** Serum blood urea nitrogen (BUN), with all data obtained at 12 weeks after surgery. Sal, saline solution; HRP, handle-region peptide; 0.01, 0.01 mg·kg^{-1}·d^{-1}; 0.3, 0.3 mg·kg^{-1}·d^{-1}. *P < .05 versus the saline solution–treated sham-operated group. **(C)** Comparison of the blood pressure and indicated cardiac parameters assessed by echocardiography before (Pre) and after (Post) treatment. Neph, Nephrectomy; SBP, Systolic blood pressure; LVDd, left ventricular diastolic diameter; EF, left ventricular ejection fraction; HR, heart rate. *P < .05 versus the respective Pre value. **(D)** Cardiac function assessed by means of cardiac catheterization. *P < .05 versus the saline solution–treated sham-operated group; †P < .05 versus the

Table 1. Cardiac Function During Physiologic Examinations Before and After Treatment (8 and 12 Weeks After Surgery, Respectively)

	Sham			5/6 Nephrectomy		
Measure	Saline (n = 10)	HRP 0.01 mg/kg (n = 6)	HRP 0.3 mg/kg (n = 10)	Saline (n = 10)	HRP 0.01 mg/kg (n = 6)	HRP 0.3 mg/kg (n = 10)
Before treatment						
LVEDd, mm	3.2 ± 0.03	3.2 ± 0.03	3.2 ± 0.03	3.5 ± 0.07*	3.5 ± 0.05*	3.5 ± 0.06*
LVEF, %	74 ± 1.8	76 ± 2.7	77 ± 1.5	66 ± 3.5*	66 ± 1.1*	66 ± 6.2*
SBP, mm Hg	104 ± 6.0	104 ± 5.8	103 ± 3.4	112 ± 7.9*	112 ± 4.1*	112 ± 9.1*
Heart rate, beats/min	637 ± 39	634 ± 64	648 ± 28	668 ± 54	662 ± 45	661 ± 46
After treatment						
LVEDd, mm	3.2 ± 0.05	3.2 ± 0.05	3.2 ± 0.02	3.7 ± 0.14*,‡	3.6 ± 0.17*,‡	3.4 ± 0.06*,†,‡
LVEF, %	75 ± 1.4	74 ± 0.86	75 ± 3.6	65 ± 4.0*	66 ± 2.0*	74 ± 1.7*,†,‡
SBP, mm Hg	104 ± 6.0	104 ± 4.1	103 ± 5.2	115 ± 7.4*	114 ± 9.1*	102 ± 8.2†,‡
Heart rate, beats/min	654 ± 51	655 ± 55	652 ± 66	684 ± 19	664 ± 51	684 ± 26

HRP, handle-region peptide; LVEDd, left ventricular end-diastolic diameter; LVEF, left ventricular ejection fraction; SBP, systolic blood pressure.
*P < 0.05 versus the saline solution−treated sham-operated group.
†$P < .05$ vs the saline solution−treated 5/6 nephrectomy group.
‡$P < 0.05$ vs the corresponding pretreatment value.

Downstream Mediators of (P)RR in the Heart

ERK, p38MAPK, and HSP27 are known downstream mediators of (P)RR signaling pathways in cardiac cells.[11,13] Western blotting analysis revealed that phosphorylation of ERK, p38, and HSP27 were enhanced in the hearts from nephrectomized mice, whereas these levels of phosphorylation were significantly suppressed in HRP-treated mice (Fig. 5).

Autophagy Findings in the Heart

Next, we examined the effects of pharmacologic (P)RR blockade with the use of HRP on autophagy in the heart, because genetically (P)RR-depleted cardiomyocytes are highly vacuolized and show impaired autophagic degradation.[10,15] The number of GFP-positive autophagic vacuoles was significantly increased within cardiomyocytes from nephrectomized GFP-LC3 transgenic mice compared with sham-operated mice, and was not affected by HRP-treatment (Fig. 6A). Western blotting analysis showed that LC3-II was up-regulated more in nephrectomized mouse hearts. As a result, the LC3-II/I ratio, which is indicative of autophagic turnover,[31] was significantly increased but not affected by HRP treatment (Fig. 6B). The level of cathepsin D, a lysosomal protein, was increased more in nephrectomized mouse hearts than in sham-operated but was not affected by HRP treatment (Fig. 6B). In addition, we examined protein levels of V-ATPase, because V-ATPase colocalized with (P)RR distributes on the vesicular membrane of the lysosome and regulates acidification in vesicles.[10] The expression level of V-ATPase was significantly increased in nephrectomized mouse hearts compared with sham-operated and was not affected by HRP treatment (Fig. 6B). Finally, electron microscopy revealed that both autophagic vacuoles and lysosomes were abundant within cardiomyocytes from nephrectomized mouse hearts and not affected by HRP treatment (Fig. 6C). These ultrastructural findings are consistent with the results of immunohistochemistry and Western blotting analysis. Overall, these findings indicate that autophagic activity was rather augmented in the hearts of nephrectomized mice but unaffected by (P)RR blockade on HRP treatment.

Discussion

The recent discovery of (P)RR has provided new insight into the mechanisms of cardiac remodeling. The present study is the first to demonstrate that (P)RR blockade ameliorated CKD-associated heart failure accompanied by the attenuation of cardiac fibrosis and hypertrophy without harmful side-effects.

Significant renal dysfunction and increased SBP were observed in mice after five-sixths nephrectomy. Nephrectomy also induced marked LV remodeling (dilated cavity and LVH) and dysfunction accompanied by cardiomyocyte hypertrophy, myocardial interstitial fibrosis, macrophage infiltration, and oxidative damage. Notably, HRP treatment significantly lowered SBP and partially reversed LV remodeling and improved cardiac performance.

Possible Mechanisms Underlying Favorable Effects of (P)RR Blockade

In the present study, nephrectomized mice exhibited significant SBP elevation, although HRP-treated mice showed lower SBP and ameliorated cardiac dysfunction. The reduction in SBP observed after (P)RR blockade is consistent with earlier studies of pacing-induced heart failure[20] and cardiac remodeling after myocardial infarction.[21] We previously demonstrated that a decline in blood pressure with the use of hydralazine did not improve the cardiac function and

saline solution−treated nephrectomy group. LVSP, left ventricular peak systolic pressure; LVEDP, left ventricular end-diastolic pressure; +dP/dt and −dP/dt, maximal and minimal first derivative of left ventricular pressure. n = 10 for saline treatment n = 6 for low-dose HRP treatment, and n = 10 for high-dose HRP treatment with each sham operation and nephrectomy, respectively.

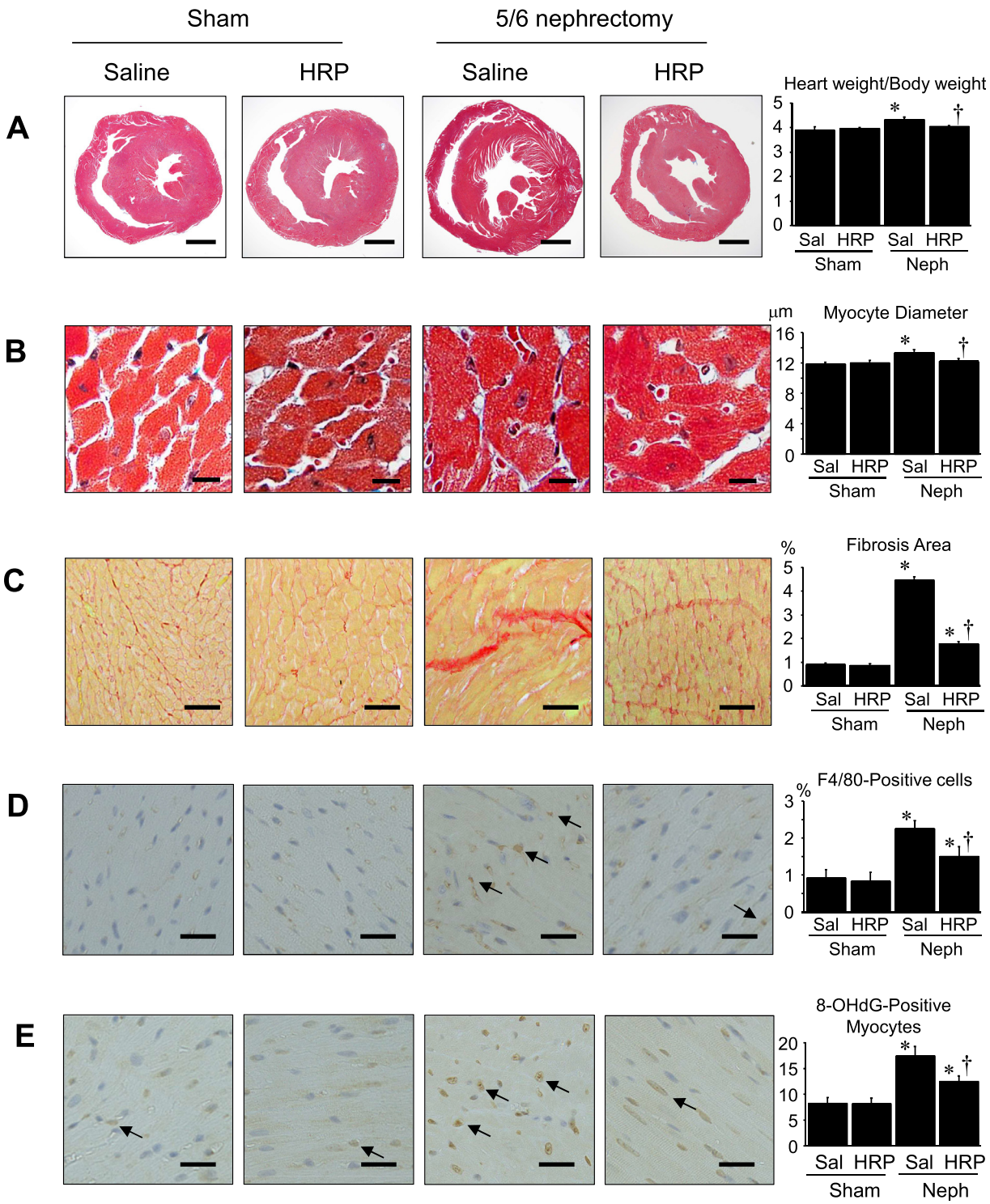

Fig. 2. Histology and immunohistochemistry of the heart. **(A)** Transverse ventricular section and **(B)** Representative micrographs of cardiomyocytes stained with Masson trichrome staining. **(C)** Interstitial myocardial fibrosis visualized by staining with Sirius red. **(D)** Macrophage infiltration (*arrows*) visualized by anti-F4/80 immunostaining. **(E)** Oxidative deoxyribonucleic acid damage (*arrows*) visualized by anti−8-OHdG immunostaining. Each graph shows quantitative morphometry (n = 10 for each). Scale bars: 1 mm in **A**; 10 μm in **B**; 40 μm in **C**; 20 μm in D and E. Abbreviations as in Fig. 1. *$P < .05$ versus the saline solution−treated sham-operated group; †$P < .05$ versus the saline solution−treated nephrectomy group.

altered the molecular signaling in the nephrectomized animal model.[9] In clinical studies of end-stage CKD patients with hypertension, Shibasaki et al reported that losartan (an AT1R antagonist), enalapril (an angiotensin-converting enzyme inhibitor), and amlodipine (a calcium antagonist) led to similar significant decreases in the mean blood pressure, but only losartan suppressed left ventricular hypertrophy.[32] Thus, these previous reports indicate that blood

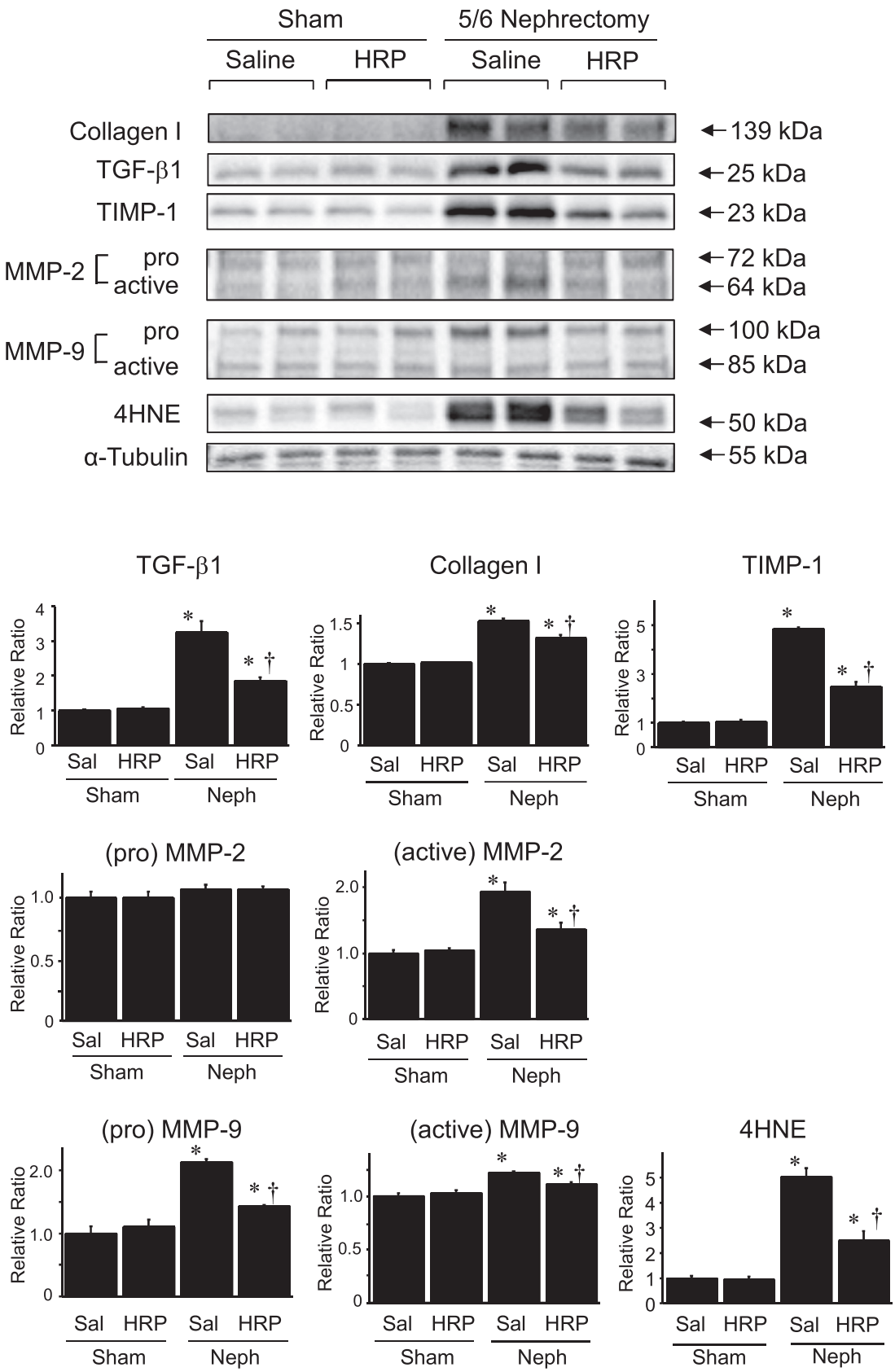

Fig. 3. Fibrosis and lipid peroxidation in the heart. Western blotting with densitometric analysis of collagen I, TGF-β1, MMP-2, MMP-9, TIMP-1, and 4-HNE in hearts at 12 weeks after surgery (n = 6 for each). *$P < .05$ versus the saline-treated sham-operated group, †$P < .05$ versus the saline-treated nephrectomy group. TGF, transforming growth factor; MMP, matrix metalloproteinase; TIMP, tissue inhibitor of metalloproteinase; 4-HNE, 4-hydroxyl-2-nonenal; other abbreviations as in Table 1.

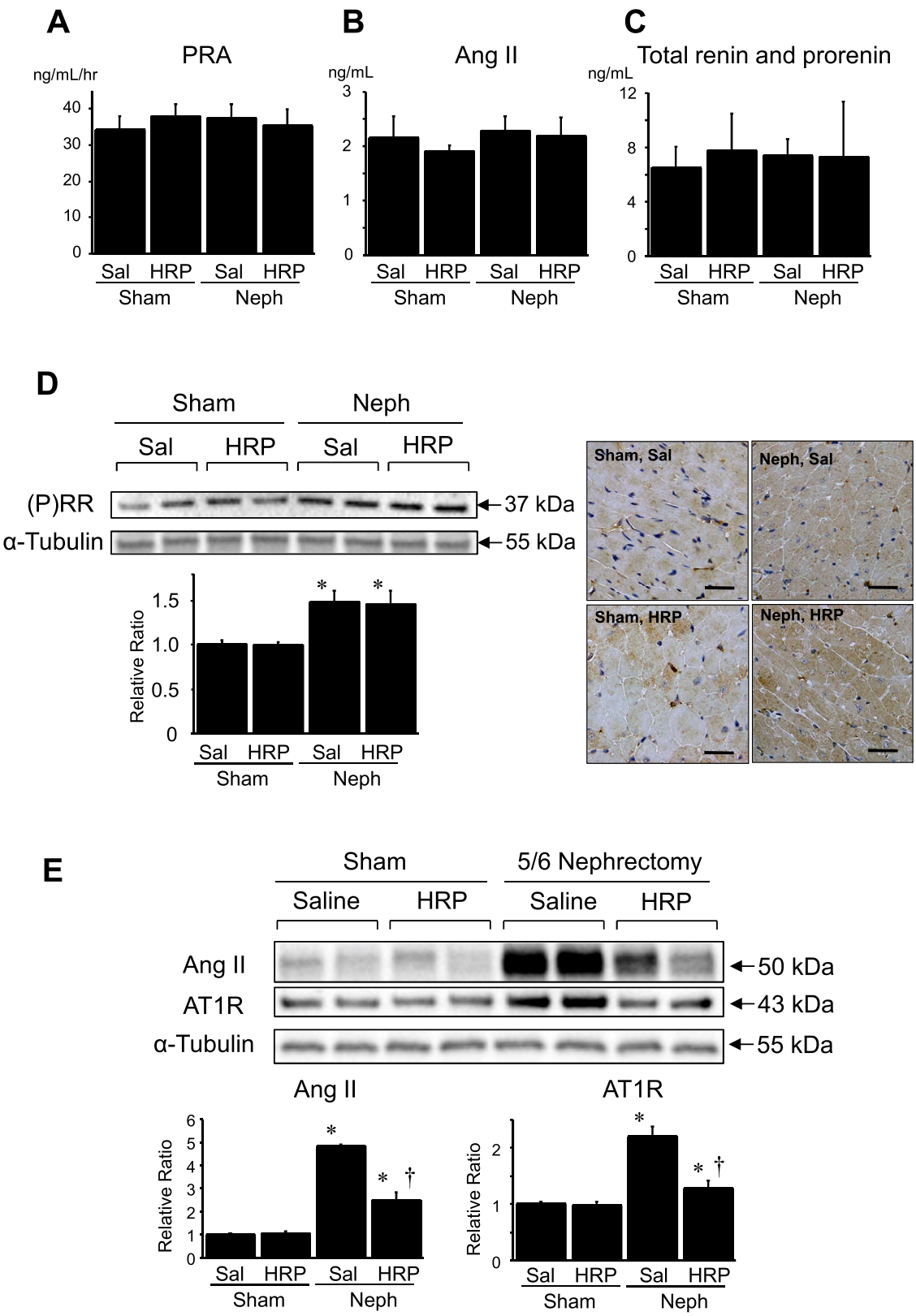

Fig. 4. Assessment of renin-angiotensin system (RAS) , prorenin, and (pro)renin receptor [(P)RR]. **(A)** Plasma renin activity, **(B)** plasma angiotensin (Ang) II, **(C)** plasma renin-prorenin (n = 6 for each). **(D)** (P)RR expression in heart tissue; right panel shows representative immunohistochemical staining for (P)RR, brown positive, scale bars = 20 μm; left panel shows Western blotting with densitometric analysis of (P)RR (n = 6 for each). **(E)** Western blotting with densitometric analysis of Ang II and Ang II type 1 receptor (AT1R) in heart tissue (n = 6 for each). *$P < .05$ versus the saline solution−treated sham-operated group; †$P < .05$ versus the saline solution−treated nephrectomy group. Other abbreviations as in Fig. 1.

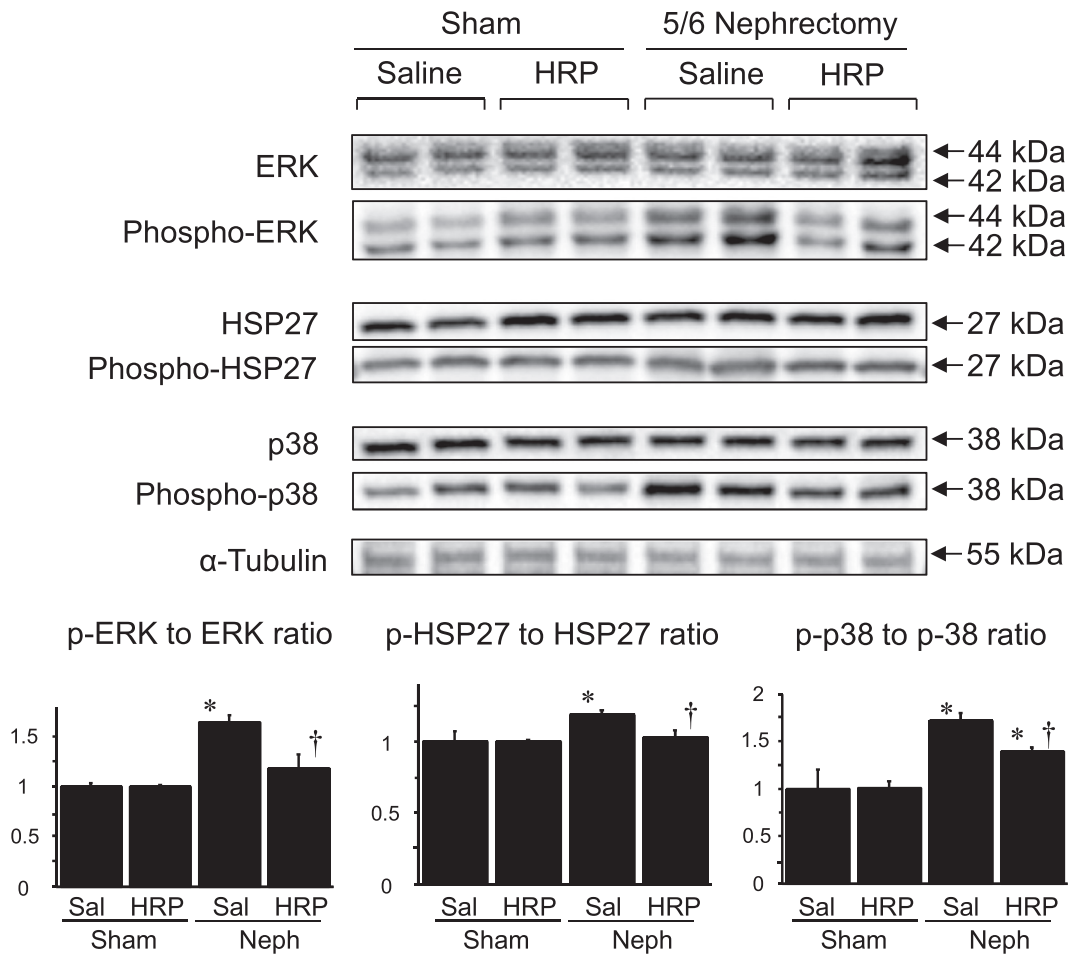

Fig. 5. Western blotting with densitometric analysis of the downstream mediators of the (pro)renin receptor; extracellular signal−regulated protein kinase (ERK), p38 mitogen−activated protein kinase (p38), heat shock protein (HSP) 27, and their phosphorylation forms in the heart tissue (n = 6 for each). *$P < .05$ versus the saline solution−treated sham-operated group; †$P < .05$ versus the saline solution−treated nephrectomy group. Other abbreviations as in Fig. 1.

pressure control alone was insufficient to alter cardiac remodeling. Therefore, we suggest that the beneficial effects of (P)RR blockade on the cardiac function were independent from its pure antihypertensive effect.

When prorenin binds to (P)RR, the prosegment covering the active site of prorenin, namely the "handle region," becomes unfolded, and the enzymatic cleft is exposed. This nonproteolytically activated prorenin can generate Ang I from angiotensinogen locally, and subsequently produce Ang II, thereby activating the tissue RAS.[11,12] In the present study, PRA, plasma Ang II, and plasma renin-prorenin concentrations were not different between sham-operated and nephrectomized mice with or without HRP treatment. These findings are consistent with previous reports: PRA levels after five-sixths nephrectomy were not different from sham-operated rodents,[33,34] and serum prorenin levels did not correlate with parameters related to renal function in CKD patients.[35] On the other hand, myocardial expressions of (P)RR, Ang II, and AT1R were all significantly increased in nephrectomized mice. In addition, myocardial expressions of Ang II and AT1R were reduced in nephrectomized mice with HRP treatment. These findings suggest that the heart tissue RAS, but not circulating RAS, was activated in the CKD mice and partially depended on modulating (P)RR. In response to Ang II stimulation, AT1R activates ERK signaling to induce cardiomyocyte hypertrophy.[36] Ang II, via AT1R, mediates the up-regulation of fibrosis-associated genes, including TGF-β1, collagen I, collagen III, and fibronectin, in cardiac fibroblasts.[7] Although the signaling cascade of fibrosis in cardiac fibroblasts remains unclear, recent studies suggested that Ang II activates AT1R/p38MAPK signaling and subsequently increases TGF-β1 expression in skeletal muscle cells or pancreatic stellate cells.[37,38] Thus, (P)RR blockade may reduce local Ang II generation and subsequently tissue RAS activation involving ERK/p38MAPK via AT1R, and consequently attenuate its deleterious downstream effects, such as fibrosis or hypertrophy, in the CKD heart.

In addition, it is considered that another mechanism exists to block fibrosis or cardiomyocyte hypertrophy via (P)RR directly. (P)RR has been reported to exert Ang II−independent effects by the activation of an intracellular postreceptor cascade: ERK activation leads to the up-regulation of TGF-β1, which induces fibrosis molecules

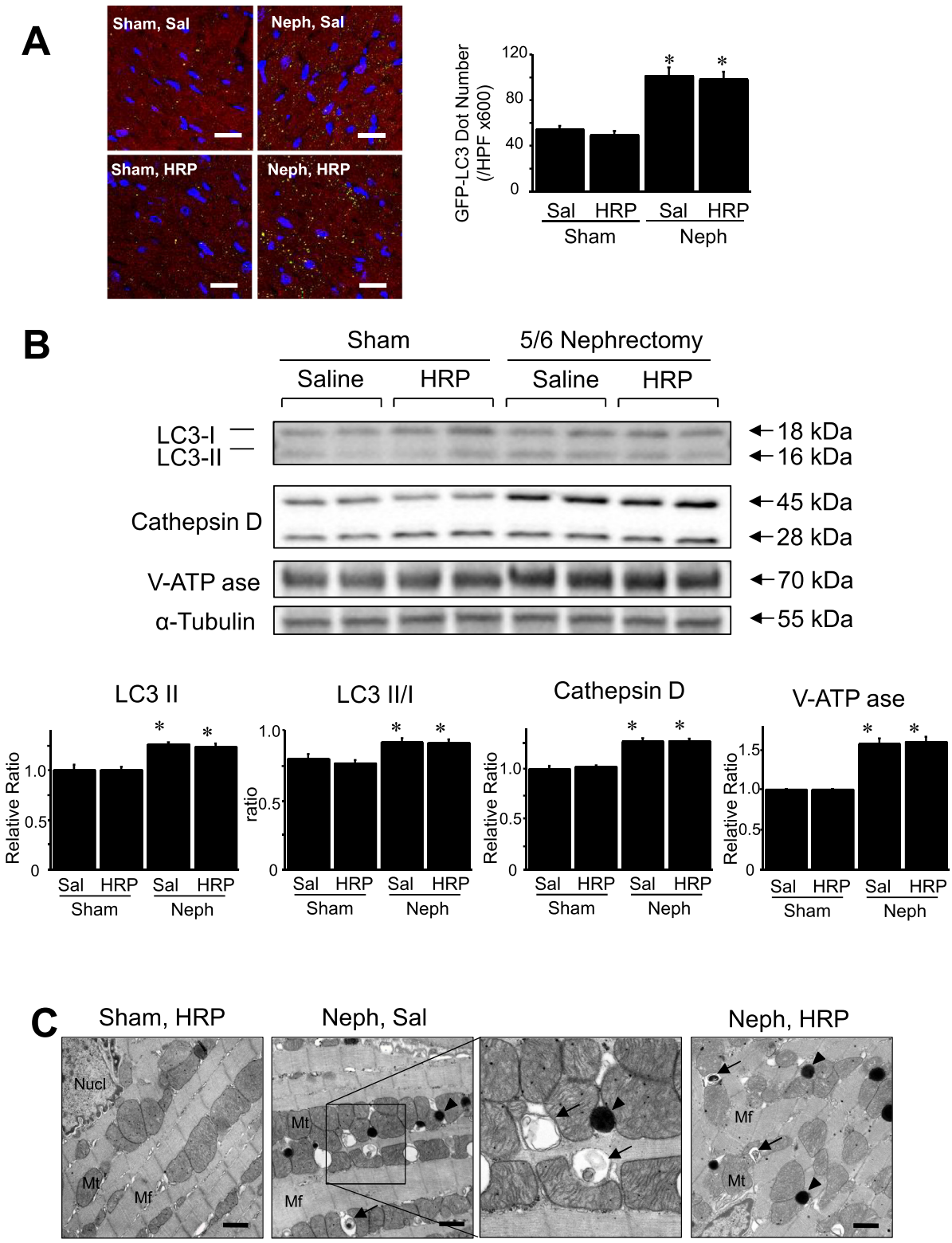

Fig. 6. Autophagy in the heart. **(A)** Immunofluorescent labeling of GFP-LC3 (*green dots*) and myoglobin (*red*) with cardiomyocytes and nuclei stained by Hoechst 33342 (*blue*) from GFP-LC3 transgenic mice. Scale bars = 20 μm. The graph shows the number of GFP-LC3 dots per high-power field (HPF). **(B)** Western blotting with densitometric analysis of LC3, cathepsin D, and V-ATPase. Graphs show the intensity of each band in arbitrary units and the LC3-II/I ratio (n = 6 for each). **(C)** Electron micrographs of autophagic vacuoles in cardiomyocytes. Arrowheads and arrows indicate lysosomes (electron-dense spherical bodies) and autophagic vacuoles. Scale bars = 1 μm. Mt, mitochondria; Mf, myofibril; Nucl, nucleus. *$P < .05$ versus the saline solution−treated sham-operated group, †$P < .05$ versus the saline solution−treated nephrectomy group. Other abbreviations as in Fig. 1.

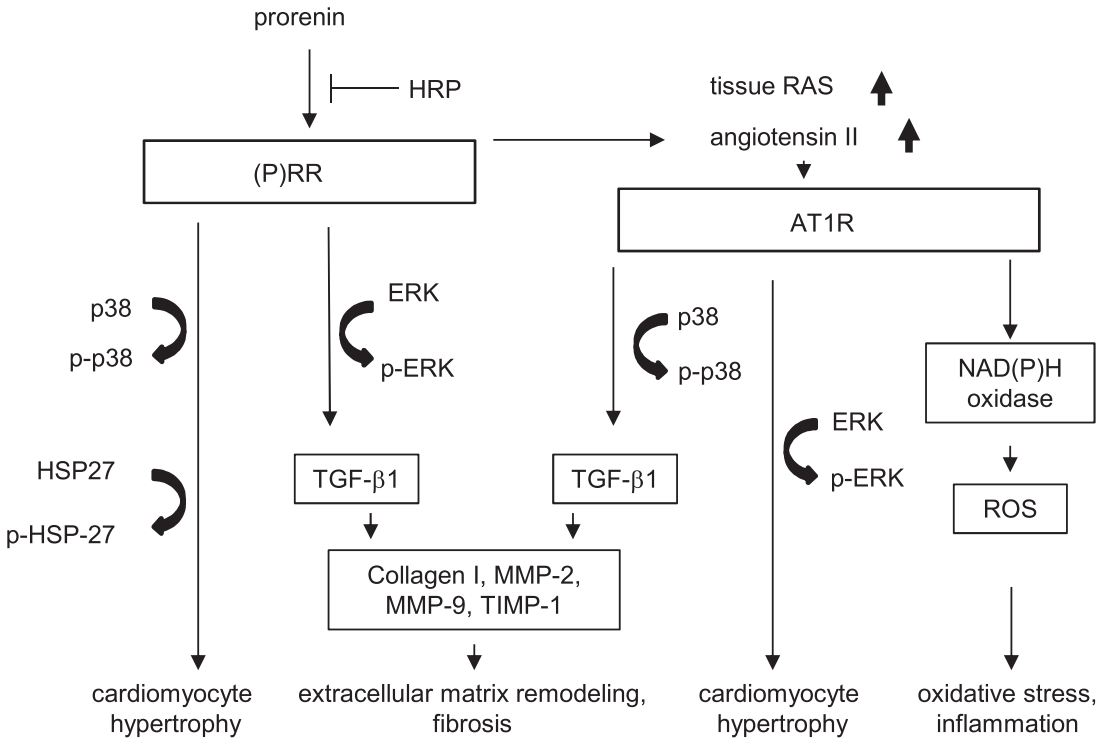

Fig. 7. Proposed scheme showing a possible link of signal transduction between the (P)RR system and tissue RAS in chronic kidney disease−associated heart failure. (P)RR blockade with the use of HRP may exert an effect on cardioprotection through the inhibition of both signal transductions. ROS, Reactive oxygen species; other abbreviations as in Fig. 3 and 5.

including fibronectin, plasminogen activator inhibitor 1, collagen I, and collagen III[39]; P38MAPK/HSP27 pathway activation enhances the synthesis of DNA and induces cardiomyocyte hypertrophy.[13] In the present study, ERK, p38MAPK, and HSP27 were all significantly phosphorylated in the nephrectomized mouse hearts and were suppressed by HRP treatment. These phosphorylations paralleled cardiac fibrosis and cardiomyocyte hypertrophy.

Myocardial fibrosis is mediated by TGF-β1 through ECM remodeling. TGF-β1 modulates the downstream molecules including MMPs and/or TIMP, and increases collagen synthesis increase and reduces collagen degradation, leading to myocardial fibrosis.[29] In the heart of nephrectomized mice, collagen I, TGF-β1, TIMP-1, MMP-2, and MMP-9 were significantly up-regulated to increase fibrosis. When accompanied with HRP treatment, collagen I, TGF-β1, and TIMP-1 were much less up-regulated, active forms of MMP-2 and MMP-9 slightly suppressed, and cardiac fibrosis decreased.

Partial nephrectomy led to myocardial oxidative damage detected by means of 8-OHdG or 4-HNE expression and inflammatory reaction with macrophage infiltration, both suppressed by HRP treatment. When Ang II acts through AT1R, it stimulates the generation of superoxide, a reactive oxygen species (ROS), by NAD(P)H oxidase within vascular smooth muscle cells, cardiomyocytes, and renal tubular epithelial cells.[40−42] ROS have many unfavorable effects in living tissues and increase the levels of inflammatory cytokines, leading to the development of a vicious cycle in the failing heart. Figure 7 summarizes the proposed mechanism of (P)RR blockade in the CKD heart.

Several reports agree with beneficial effect of (P)RR blockade with the use of HRP. Long-term (P)RR blockade improved cardiac function and reduced cardiac fibrosis in salt-fed spontaneously hypertensive rats,[17,18] ameliorated postinfarction heart size, cardiac fibrosis/hypertrophy, and cardiac dysfunction.[21] In contrast, Muller et al reported that (P)RR blockade with the use of HRP does not affect blood pressure, cardiac hypertrophy, or renal damage in renovascular hypertensive rats.[19] Fukushima et al reported that (P)RR blockade did not affect the infarct size or cardiac function after coronary artery ligation, but it ameliorated insulin resistance associated with heart failure by improving insulin signaling via the inhibition of oxidative stress in skeletal muscle.[22] It is very difficult to reconcile these contradictory and complicated results, but one possibility is that the difference might be related to the methods and animal models of the studies. Because the effectiveness of HRP in vivo is controversial, partly because of the wide variety of doses applied (from 0.1 mg/kg per 28 days to 1.0 $mg \cdot kg^{-1} \cdot d^{-1}$),[43] we used 2 doses of HRP (0.01 and 0.3 $mg \cdot kg^{-1} \cdot d^{-1}$). Our results showed that the high-dose but not the low-dose HRP was effective. The dose used in the study with negative results was lower than our high-dose HRP. To identify the optimal dose to acquire an optimal effect, a detailed dose escalation study is necessary. Also, the experimental model,

renovascular hypertension, used by Muller et al showed extremely high PRA. This active renin still generates Ang II without binding to (P)RR, therefore (P)RR blockade may not show benefits under such a high-renin condition.

The (P)RR Blockade Did Not Interfere With Autophagy

Recent studies have indicated an important relationship between (P)RR and V-ATPase independent out of RAS. V-ATPase colocalized with (P)RR is distributed not only in the plasma membrane but also within organelles, such as endosomes or lysosomes,[10] and plays a pivotal role in the control of intracellular and intraorganellar pH.[44] Thus, (P)RR is considered to be involved in autophagy, an essential lysosomal degradation pathway for survival, differentiation, and development.[14,45] In fact, both cardiomyocytes[15] and podocytes[46] with the (P)RR gene ablated are highly vacuolated and show impaired autophagic degradation. However, whether HRP affects the connection between (P)RR and V-ATPase is currently unknown. At first, we were apprehensive that (P)RR blockade with the use of HRP might be detrimental due to impaired autophagy. But in the present study, autophagy was activated in the CKD mouse heart, characterized by increase in LC3-II, LC3 II/I ratio, cathepsin D, and autophagic vacuole number in cardiomyocytes. These findings did not differ with or without HRP treatment. Autophagy is generally activated in the failing heart to compensate for a lack of energy for maintenance of the cardiac function or cell survival, as we reported previously in nonhuman animal models, including acute myocardial infarction,[47] postinfarction LV remodeling,[48] and diabetic cardiomyopathy.[25] Thus, HRP showed beneficial effects of (P)RR blockade without interfering with autophagy.

Study Limitations

There are limitations in the present study that should be acknowledged. First, the treatment with HRP led to the attenuation of cardiomyocyte hypertrophy, reduced fibrosis, macrophage infiltration, and oxidative damage in the CKD hearts. However, it is difficult to determine the cell type (including cardiomyocytes, fibroblasts, and inflammatory cells) or the action on the cells that is most responsible for the beneficial effects of HRP. Second, this study was not designed to identify the pathway, tissue RAS−dependent or −independent, that is more responsible for the beneficial effect of HRP. Although we suggested the possible signal pathways including, ERK, p38, and HSP27 based on our results and previous reports, we could not conclude the main pathway owing to its complexity among various cell types. For example, matrix turnover mainly contributes to cardiac remodeling as well as cardiomyocyte hypertrophy, and it is affected by a number of cell types expressing MMPs within the myocardium, including fibroblasts, cardiomyocytes, endothelial cells, vascular smooth muscle cells, neutrophils, and macrophages.[49] These issues may be resolved with the use of conditional knockout or transgenic mice expressing RAS-related genes with HRP treatment. Further investigation is needed to explore these issues.

Clinical Implications

Angiotensin-converting enzyme inhibitors, angiotensin-receptor blockers (ARBs), β-blockers, and spironolactone are generally established agents to improve survival in patients with heart failure. However, these pharmacotherapies are not always indicated for heart failure patients with CKD because of hyperkalemia or an increased risk of adverse renal dysfunction.[50] Recently, ARBs were studied to treat heart failure clinically, but the cardioprotective effect was still insufficient. The present study demonstrated that HRP is a hopeful candidate to treat heart failure in CKD, probably owing to inhibition of unfavorable signaling pathways via both AT1R and (P)RR. Thus, our present findings provide new insights into expanded RAS-related therapeutic strategies involving (P)RR blockade for patients suffering from heart failure in the presence of renal dysfunction. The development of clinical drugs that directly block (P)RR is warranted.

Acknowledgements

The authors thank Akiko Tsujimoto, Ayaka Kanbara, Kazuho Niwa, and Akiho Kimura of Gifu Univeristy for their assistance.

Disclosures: None.

References

1. Sarnak MJ, Levey AS, Schoolwerth AC, Coresh J, Culleton B, Hamm LL, et al. American Heart Association Councils on Kidney in Cardiovascular Disease, High Blood Pressure Research, Clinical Cardiology, and Epidemiology and Prevention. Kidney disease as a risk factor for development of cardiovascular disease: a statement from the American Heart Association Councils on Kidney in Cardiovascular Disease, High Blood Pressure Research, Clinical Cardiology, and Epidemiology and Prevention. Circulation 2003;108:2154–69.
2. Foley RN, Parfrey PS, Sarnak MJ. Clinical epidemiology of cardiovascular disease in chronic renal disease. Am J Kidney Dis 1998;32(5 Suppl 3):S112–9.
3. Silberberg JS, Barre PE, Prichard SS, Sniderman AD. Impact of left ventricular hypertrophy on survival in end-stage renal disease. Kidney Int 1989;36:286–90.
4. Grossman W. Cardiac hypertrophy: useful adaptation or pathologic process? Am J Med 1980;69:576–84.
5. Tyralla K, Amann K. Cardiovascular changes in renal failure. Blood Purif 2002;20:462–5.
6. Ronco C, Haapio M, House AA, Anavekar N, Bellomo R. Cardiorenal syndrome. J Am Coll Cardiol 2008;52:1527–39.
7. Kim S, Iwao H. Molecular and cellular mechanisms of angiotensin II−mediated cardiovascular and renal diseases. Pharmacol 2000;52:11–34.
8. Sun Y. Intracardiac renin-angiotensin system and myocardial repair/remodeling following infarction. J Mol Cell Cardiol. 2010;48:483–9.
9. Li Y, Takemura G, Okada H, Miyata S, Maruyama R, Esaki M, et al. Molecular signaling mediated by angiotensin II type 1A receptor blockade leading to attenuation of renal dysfunction−associated heart failure. J Card Fail 2007;13:155–62.

10. Krop M, Lu X, Danser AH, Meima ME. The (pro)renin receptor. A decade of research: what have we learned? Pflugers Arch 2013;465:87–97.
11. Schroten NF, Gaillard CA, van Veldhuisen DJ, Szymanski MK, Hillege HL, de Boer RA. New roles for renin and prorenin in heart failure and cardiorenal crosstalk. Heart Fail Rev 2012;17:191–201.
12. Nguyen G, Delarue F, Burcklé C, Bouzhir L, Giller T, Sraer JD. Pivotal role of the renin/prorenin receptor in angiotensin II production and cellular responses to renin. J Clin Invest 2002;109:1417–27.
13. Saris JJ, 't Hoen PA, Garrelds IM, Dekkers DH, den Dunnen JT, Lamers JM, et al. Prorenin induces intracellular signaling in cardiomyocytes independently of angiotensin II. Hypertension 2006;48:564–71.
14. Loos B, Engelbrecht AM, Lockshin RA, Klionsky DJ, Zakeri Z. The variability of autophagy and cell death susceptibility: unanswered questions. Autophagy 2013;9:1270–85.
15. Kinouchi K, Ichihara A, Sano M, Sun-Wada GH, Wada Y, Kurauchi-Mito A, et al. The (pro)renin receptor/ATP6AP2 is essential for vacuolar H^+-ATPase assembly in murine cardiomyocytes. Circ Res 2010;107:30–4.
16. Ichihara A, Hayashi M, Kaneshiro Y, Suzuki F, Nakagawa T, Tada Y, et al. Inhibition of diabetic nephropathy by a decoy peptide corresponding to the "handle" region for nonproteolytic activation of prorenin. J Clin Invest 2004;114:1128–35.
17. Ichihara A, Kaneshiro Y, Takemitsu T, Sakoda M, Suzuki F, Nakagawa T, et al. Nonproteolytic activation of prorenin contributes to development of cardiac fibrosis in genetic hypertension. Hypertension 2006;47:894–900.
18. Susic D, Zhou X, Frohlich ED, Lippton H, Knight M. Cardiovascular effects of prorenin blockade in genetically spontaneously hypertensive rats on normal and high-salt diet. Am J Physiol Heart Circ Physiol 2008;295:H1117–21.
19. Muller DN, Klanke B, Feldt S, Cordasic N, Hartner A, Schmieder RE, et al. (Pro)renin receptor peptide inhibitor "handle-region" peptide does not affect hypertensive nephrosclerosis in Goldblatt rats. Hypertension 2008;51:676–81.
20. Rademaker MT, Yandle TG, Ellmers LJ, Charles CJ, Nicholls MG, Richards AM. Hemodynamic, hormonal, and renal effects of (pro)renin receptor blockade in experimental heart failure. Circ Heart Fail 2012;5:645–52.
21. Ellmers LJ, Rademaker MT, Charles CJ, Yandle TG, Richards AM. (Pro)renin receptor blockade ameliorates cardiac injury and remodeling and improves function after myocardial infarction. J Card Fail 2016;22:64–72.
22. Fukushima A, Kinugawa S, Takada S, Matsushima S, Sobirin MA, Ono T, et al. (Pro)renin receptor in skeletal muscle is involved in the development of insulin resistance associated with postinfarct heart failure in mice. Am J Physiol Endocrinol Metab 2014;307:E503–14.
23. Ichihara A, Sakoda M, Kurauchi-Mito A, Nishiyama A, Itoh H. Involvement of receptor-bound prorenin in development of nephropathy in diabetic db/db mice. J Am Soc Hypertens 2008;2:332–40.
24. Mizushima N, Yamamoto A, Matsui M, Yoshimori T, Ohsumi Y. In vivo analysis of autophagy in response to nutrient starvation using transgenic mice expressing a fluorescent autophagosome marker. Mol Biol Cell 2004;15:1101–11.
25. Kanamori H, Takemura G, Goto K, Tsujimoto A, Mikami A, Ogino A, et al. Autophagic adaptations in diabetic cardiomyopathy differ between type 1 and type 2 diabetes. Autophagy 2015;11:1146–60.
26. Uegaito T, Fujiwara H, Ishida M, Kawamura A, Takemura G, Kida M, et al. Hypertrophy of surviving myocytes overlying the infarct in human old myocardial infarctions with abnormal Q waves. Int J Cardiol 1991;32:93–101.
27. Toyokuni S, Tanaka T, Hattori Y, Nishiyama Y, Yoshida A, Uchida K, et al. Quantitative immunohistochemical determination of 8-hydroxy-2′-deoxyguanosine by a monoclonal antibody N45.1: its application to ferric nitrilotriacetate-induced renal carcinogenesis model. Lab Invest 1997;76:365–74.
28. Leask A. Potential therapeutic targets for cardiac fibrosis: TGFbeta, angiotensin, endothelin, CCN2, and PDGF, partners in fibroblast activation. Circ Res 2010;106:1675–80.
29. Spinale FG. Matrix metalloproteinases: regulation and dysregulation in the failing heart. Circ Res 2002;90:520–30.
30. Toyokuni S, Uchida K, Okamoto K, Hattori-Nakakuki Y, Hiai H, Stadtman ER. Formation of 4-hydroxy-2-nonenal−modified proteins in the renal proximal tubules of rats treated with a renal carcinogen, ferric nitrilotriacetate. Proc Natl Acad Sci U S A 1994;91:2616–20.
31. Kabeya Y, Mizushima N, Ueno T, Yamamoto A, Kirisako T, Noda T, et al. LC3, a mammalian homologue of yeast Apg8p, is localized in autophagosome membranes after processing. EMBO J 2000;19:5720–8.
32. Shibasaki Y, Masaki H, Nishiue T, Nishikawa M, Matsubara H, Iwasaka T. Angiotensin II type 1 receptor antagonist, losartan, causes regression of left ventricular hypertrophy in end-stage renal disease. Nephron 2002;90:256–61.
33. Salas SP, Giacaman A, Romero W, Downey P, Aranda E, Mezzano D, et al. Pregnant rats treated with a serotonin precursor have reduced fetal weight and lower plasma volume and kallikrein levels. Hypertension 2007;50:773–9.
34. Vaziri ND, Bai Y, Ni Z, Quiroz Y, Pandian R, Rodriguez-Iturbe B. Intra-renal angiotensin II/AT1 receptor, oxidative stress, inflammation, and progressive injury in renal mass reduction. J Pharmacol Exp Ther 2007;323:85–93.
35. Hamada K, Taniguchi Y, Shimamura Y, Inoue K, Ogata K, Ishihara M, et al. Serum level of soluble (pro)renin receptor is modulated in chronic kidney disease. Clin Exp Nephrol 2013;17:848–56.
36. Bueno OF, Molkentin JD. Involvement of extracellular signal-regulated kinases 1/2 in cardiac hypertrophy and cell death. Circ Res 2002;91:776–81.
37. Morales MG, Vazquez Y, Acuña MJ, Rivera JC, Simon F, Salas JD, et al. Angiotensin II−induced pro-fibrotic effects require p38MAPK activity and transforming growth factor beta 1 expression in skeletal muscle cells. Int J Biochem Cell Biol 2012;44:1993–2002.
38. Sakurai T, Kudo M, Fukuta N, Nakatani T, Kimura M, Park AM, et al. Involvement of angiotensin II and reactive oxygen species in pancreatic fibrosis. Pancreatology 2011;11:7–13.
39. Huang Y, Noble NA, Zhang J, Xu C, Border WA. Renin-stimulated TGF-β1 expression is regulated by a mitogen-activated protein kinase in mesangial cells. Kidney Int 2007;72:45–52.
40. Griendling KK, Minieri CA, Ollerenshaw JD, Alexander RW. Angiotensin II stimulates NADH and NADPH oxidase activity in cultured vascular smooth muscle cells. Circ Res 1994;74:1141–8.
41. Heymes C, Bendall JK, Ratajczak P, Cave AC, Samuel JL, Hasenfuss G, et al. Increased myocardial NADPH oxidase activity in human heart failure. J Am Coll Cardiol 2003;41:2164–71.
42. Vaziri ND, Dicus M, Ho ND, Boroujerdi-Rad L, Sindhu RK. Oxidative stress and dysregulation of superoxide dismutase and NADPH oxidase in renal insufficiency. Kidney Int 2003;63:179–85.
43. Campbell DJ. Critical review of prorenin and (pro)renin receptor research. Hypertension 2008;51:1259–64.
44. Forgac M. Vacuolar ATPases: rotary proton pumps in physiology and pathophysiology. Nat Rev Mol Cell Biol 2007;8:917–29.
45. Levine B, Kroemer G. Autophagy in the pathogenesis of disease. Cell 2008;132:27–42.

46. Riediger F, Quack I, Qadri F, Hartleben B, Park JK, Potthoff SA, et al. Prorenin receptor is essential for podocyte autophagy and survival. J Am Soc Nephrol. 2011;22:2193–202.
47. Kanamori H, Takemura G, Goto K, Maruyama R, Ono K, Nagao K, et al. Autophagy limits acute myocardial infarction induced by permanent coronary artery occlusion. Am J Physiol Heart Circ Physiol 2011;300:H2261–71.
48. Kanamori H, Takemura G, Goto K, Tsujimoto A, Ogino A, Takeyama T, et al. Resveratrol reverses remodeling in hearts with large, old myocardial infarctions through enhanced autophagy-activating AMP kinase pathway. Am J Pathol 2013;182:701–13.
49. DeLeon-Pennell KY, Meschiari CA, Jung M, Lindsey ML. Matrix metalloproteinases in myocardial infarction and heart failure. Prog Mol Biol Transl Sci 2017;147:75–100.
50. Nitta K. Pathogenesis and therapeutic implications of cardiorenal syndrome. Clin Exp Nephrol 2011;15:187–94.